Supplementary Material for

C2 weakens turn over frequency during melting of Fe_xC_y: insights from reactive MD simulations

Yubing Liu,[a,b,c] Kuan Lu,*[b,c] Xingchen Liu,[b,c] Jinjia Liu,[b,c,d] Wen-Ping Guo,[c] Wei Chen,[a] Qing Peng,[e] Yu-Fei Song,*[a] Yong Yang,[b,c] Yong-Wang Li,[b,c] and Xiao-Dong Wen*[b,c]

[a]State Key Laboratory of Chemical Resource Engineering, School of Chemistry, Beijing University of Chemical Technology, Beijing 100029, P. R. China

[b]State Key Laboratory of Coal Conversion, Institute of Coal Chemistry, Chinese Academy of Sciences, Taiyuan, Shanxi 030001, P.R. China

[c]National Energy Center for Coal to Clean Fuels, Synfuels China Co., Ltd., Huairou District, Beijing 101400, P. R. China

[d]University of Chinese Academy of Sciences, No. 19A Yuquan Road, Beijing 100049, P. R. China

[e]Physics Department, King Fahd University of Petroleum & Minerals, Dhahran 31261, Saudi Arabia

Contents

Fig. S1. Validation of the Lindemann determination criteria of Fe_xC_y nanoparticles.

Fig. S2. The Wulff construction of Fe_xC_y.

Fig. S3. Cubic boxes for (a) Fe_xC_y nanoparticle melting and (b) CO activation simulations.

Table S1. The melting and pre-melting temperature of Fe_xC_y nanoparticles of various sizes.

Fig. S4. Calculated (a) temperature, (b) total energy, and (c) potential energy curve of bulk Fe_5C_2.

Fig. S5. Curves of (a) potential energy and (b) density of 5nm Fe_xC_y nanoparticles with temperature.

Fig. S6. Individual atom Lindemann index variation from a lower temperature to higher of Fe_5C_2 nanoparticles, (a) 2 nm; (b) 3 nm; (c) 5 nm; (d) 8 nm.

Fig. S7. Individual atom Lindemann index variation from a lower temperature to higher of 5 nm Fe_2C nanoparticles.

Fig. S8. Individual atom Lindemann index variation from a lower temperature to higher of 5 nm Fe_3C nanoparticles.

Fig. S9. Individual atom Lindemann index variation from a lower temperature to higher of 5 nm Fe_4C nanoparticles.

Fig. S10. The structure of bulk Fe_5C_2 and the radial distribution functions obtained for bulk Fe_5C_2.

Fig. S11. (a)-(e) The mean-square displacements (MSD) and (f)-(j) the diffusion coefficient of Fe and C atoms of Fe_5C_2 nanoparticles at different temperatures.

Fig. S12. (a) The CO dissociation number and (b) the TOF value of the nanoparticles with/without C2 models.

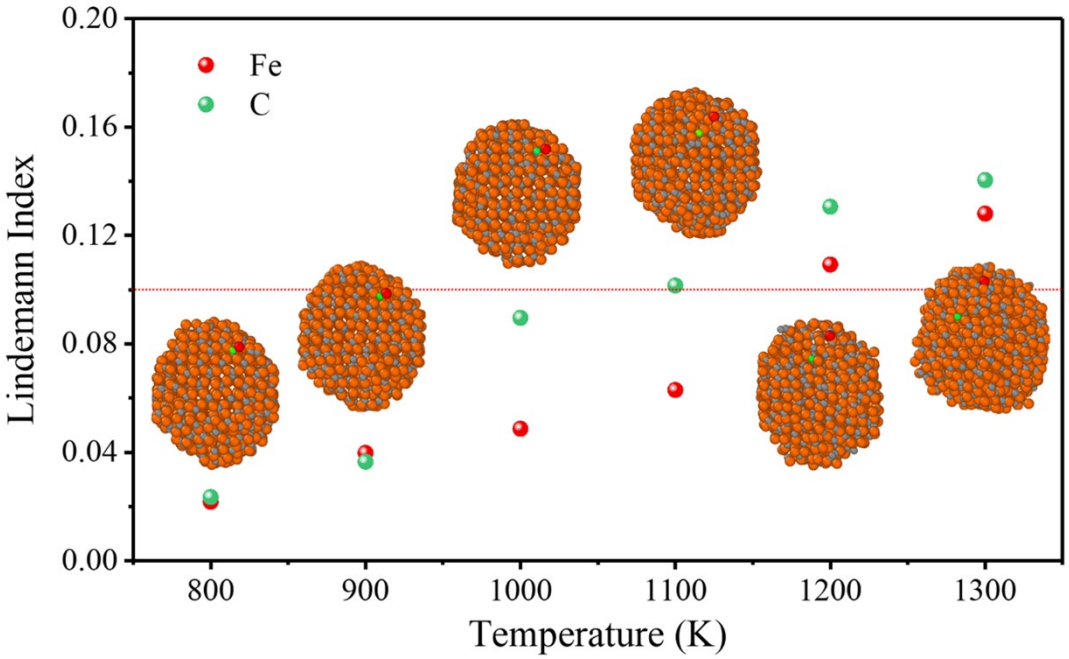

Fig. S1. Validation of the Lindemann determination criteria of Fe_xC_y nanoparticles. The figure shows the Lindemann index of the labeled atoms. The atoms are activated and diffuse when their Lindemann index reaches 0.1.

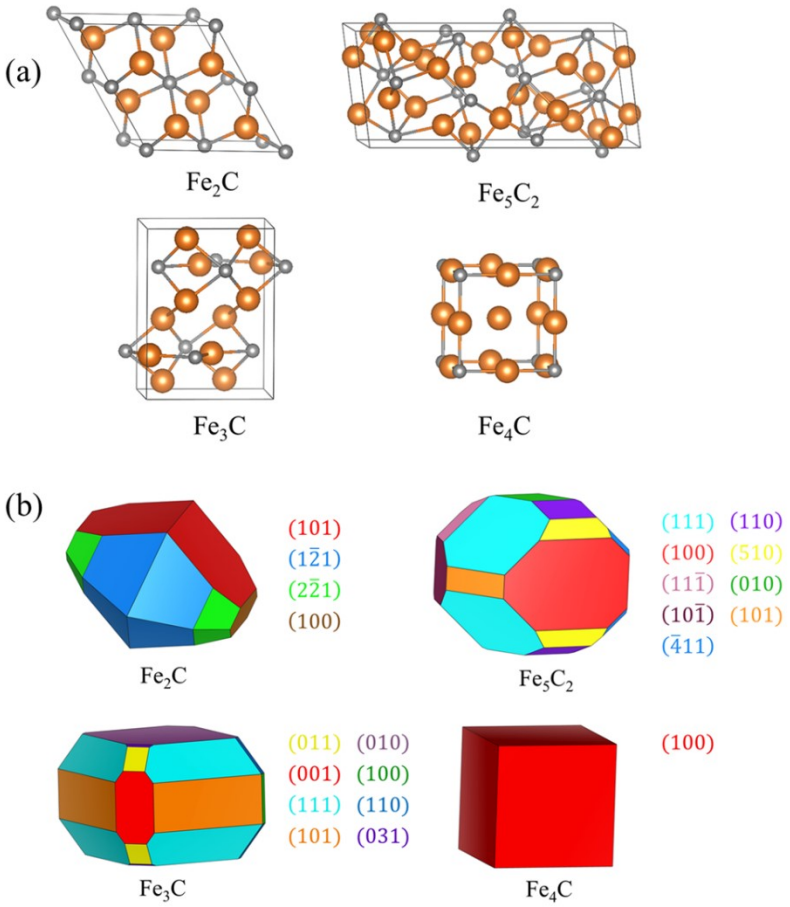

Fig. S2. (a) The initial crystal structures of Fe_xC_y; (b) the Wulff construction of Fe_xC_y.

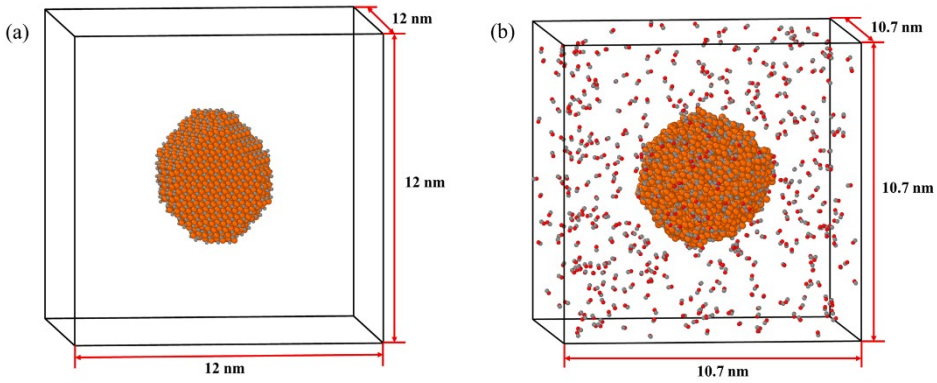

Fig. S3. Cubic boxes for (a) Fe_xC_y nanoparticle melting and (b) CO activation simulations.

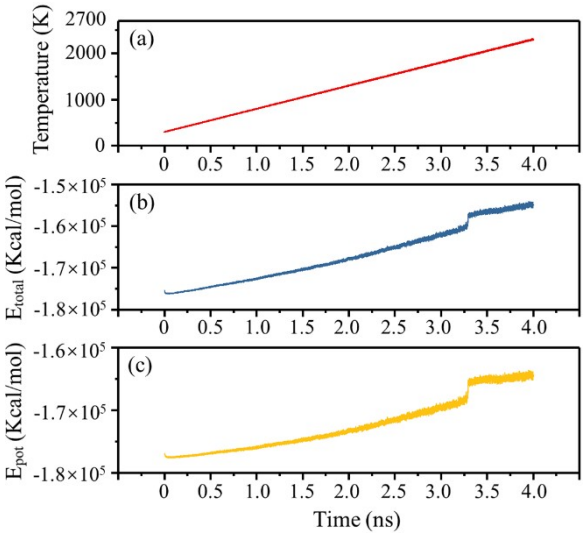

Fig. S4. Calculated (a) temperature, (b) total energy, and (c) potential energy curve of bulk Fe_5C_2.

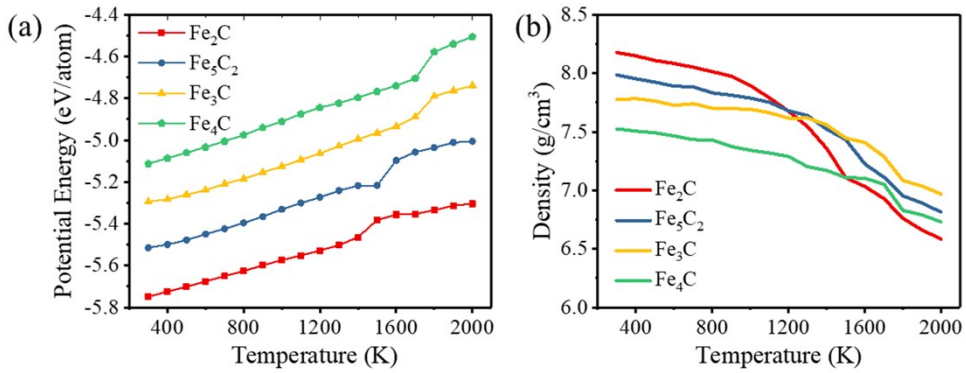

Fig. S5. Curves of (a) potential energy and (b) density of 5nm Fe_xC_y nanoparticles with temperature.

Table S1. The melting and pre-melting temperature (K) of Fe_xC_y nanoparticles of various sizes.

	Melting Temperature				Pre-melting Temperature			
	2 nm	3 nm	5 nm	8 nm	2 nm	3 nm	5 nm	8 nm
Fe_2C	1030	1275	1420	1550	850	1100	1210	1350
Fe_5C_2	1125	1380	1570	1700	850	1075	1195	1320
Fe_3C	1050	1520	1750	1875	800	1000	1095	1300
Fe_4C	950	1450	1780	1950	700	850	980	1200

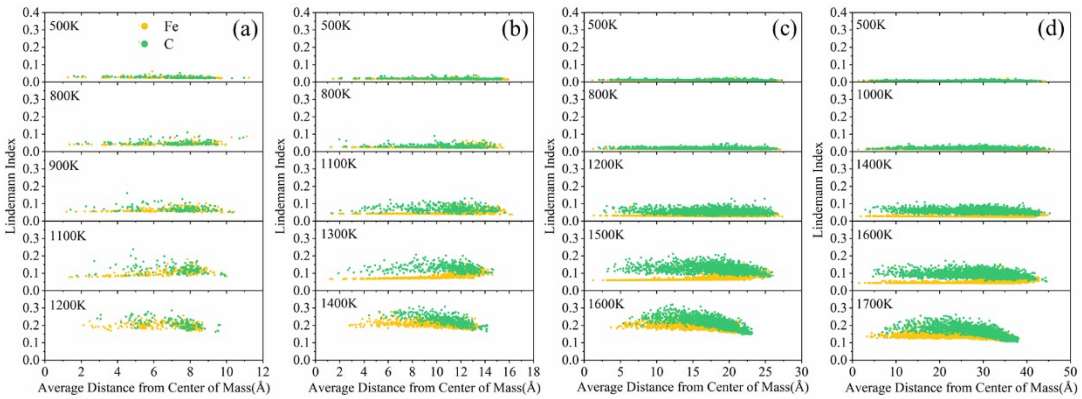

Fig. S6. Individual atom Lindemann index variation from a lower temperature to higher of Fe_5C_2 nanoparticles, (a) 2 nm; (b) 3 nm; (c) 5 nm; (d) 8 nm.

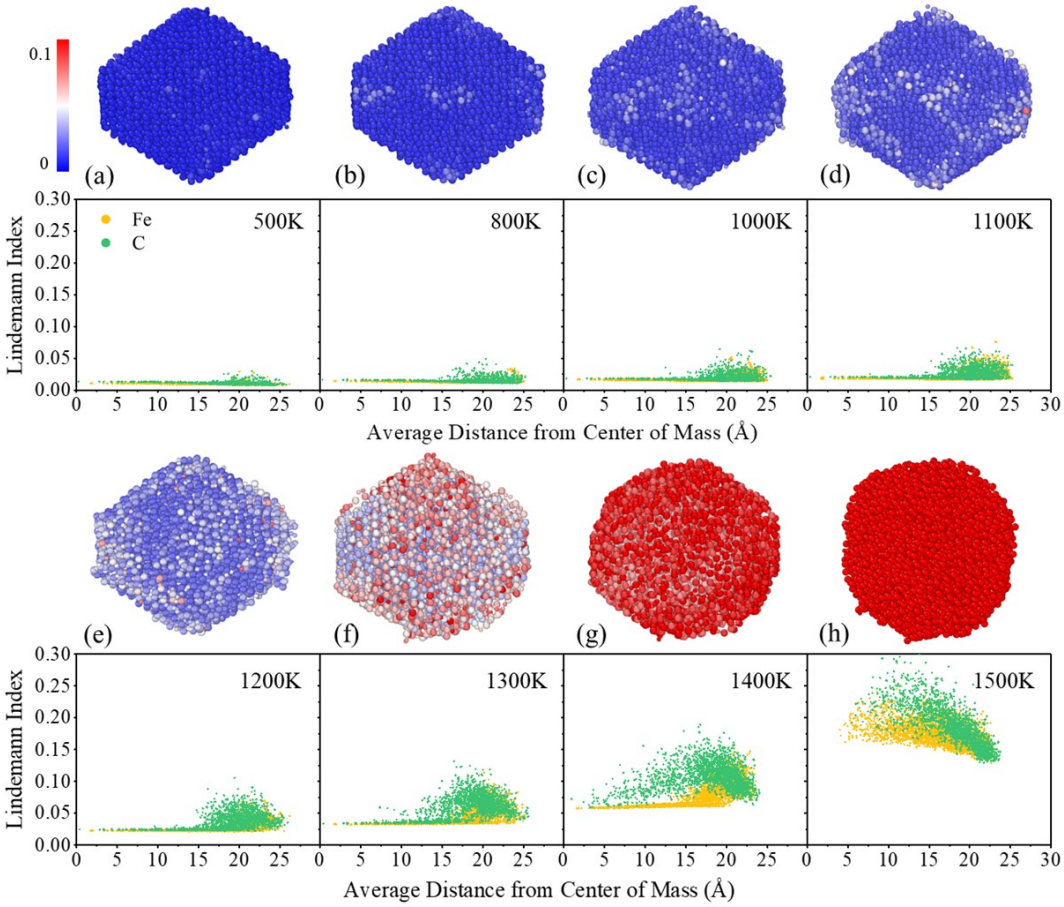

Fig. S7. Individual atom Lindemann index variation from a lower temperature to higher of 5nm Fe_2C nanoparticles.

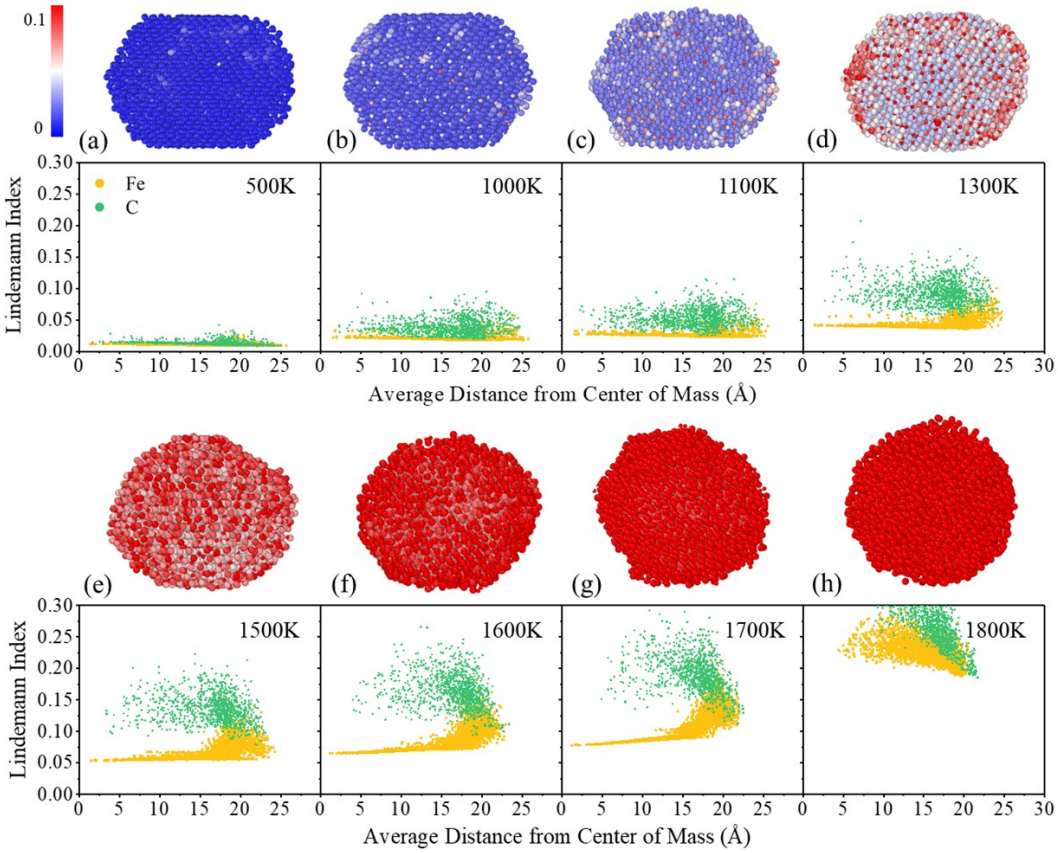

Fig. S8. Individual atom Lindemann index variation from a lower temperature to higher of 5 nm Fe_3C nanoparticles.

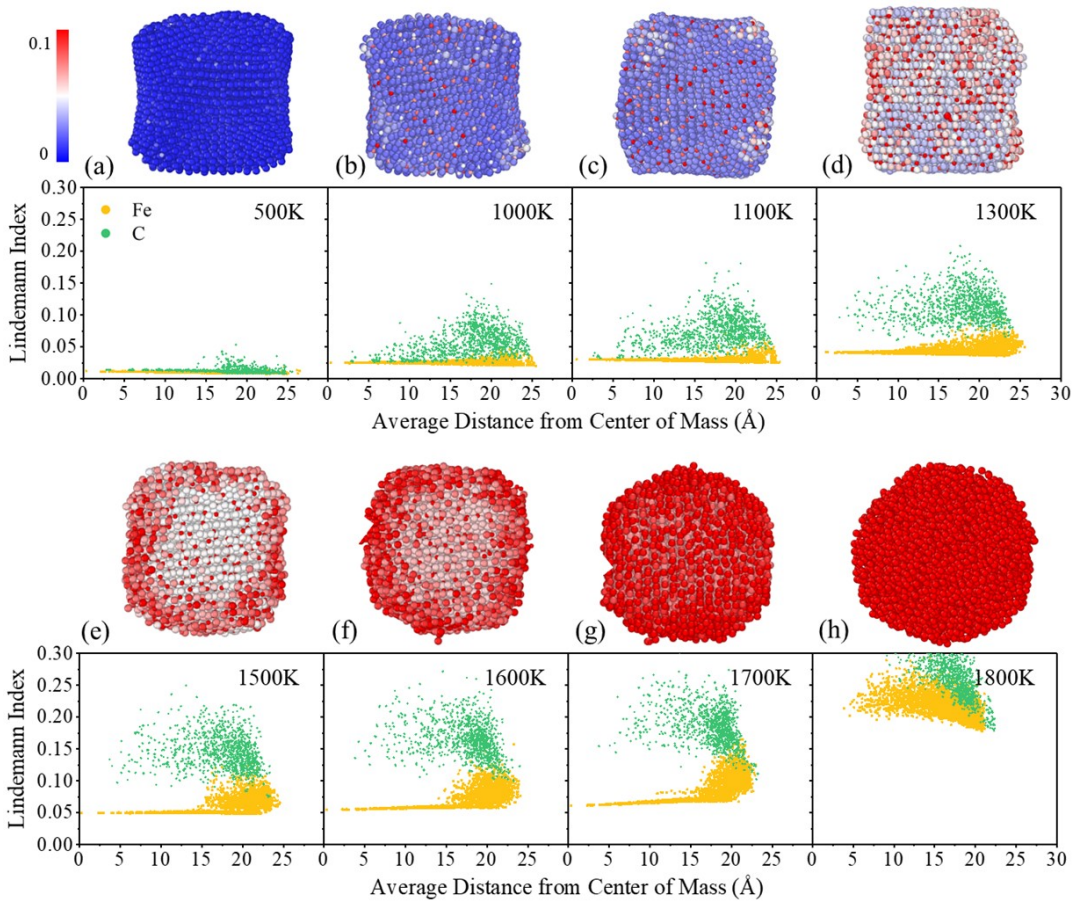

Fig. S9. Individual atom Lindemann index variation from a lower temperature to higher of 5 nm Fe_4C nanoparticles.

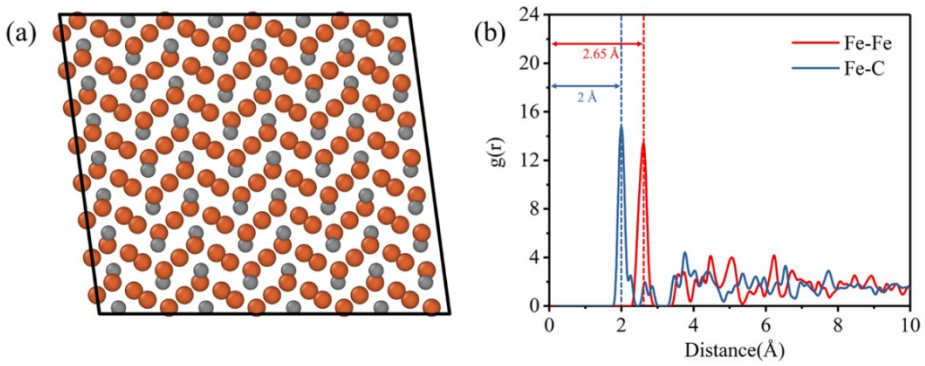

Fig. S10. (a) The structure of bulk Fe_5C_2; (b) Radial distribution functions obtained for bulk Fe_5C_2.

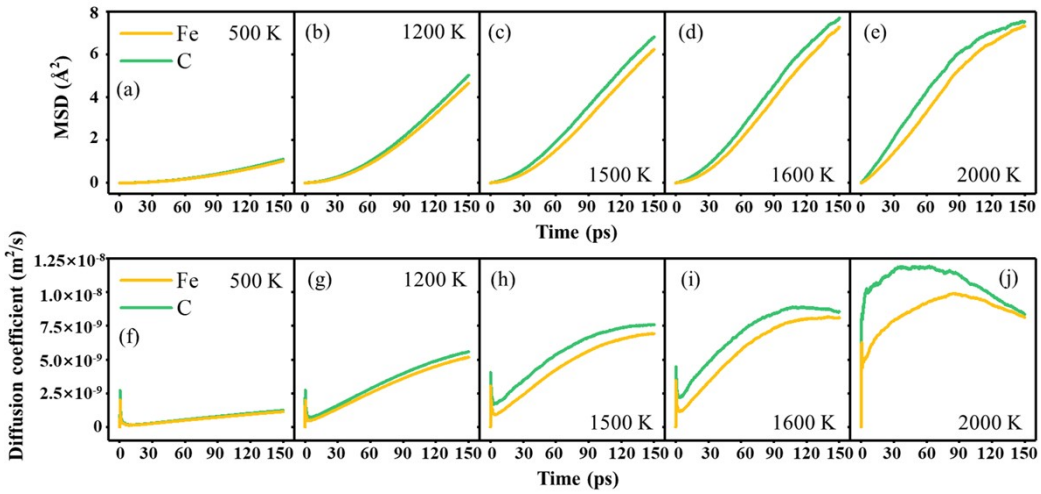

Fig. S11. (a)-(e) The mean-square displacements (MSD) and (f)-(j) the diffusion coefficient of Fe and C atoms of Fe_5C_2 nanoparticles at different temperatures.

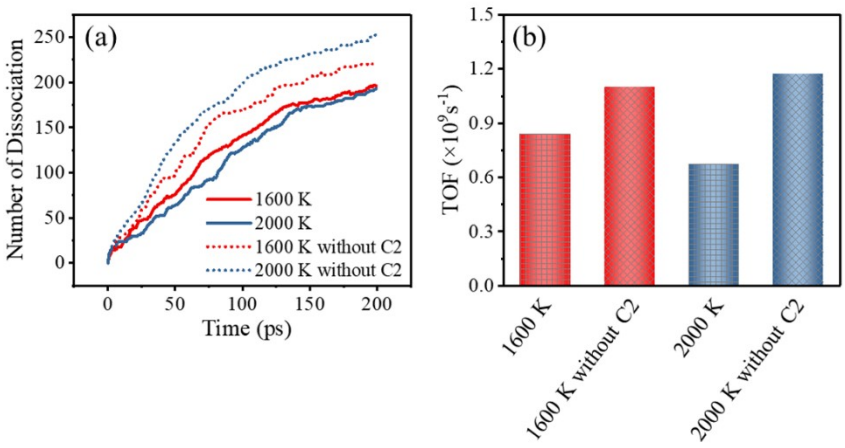

Fig. S12. (a) The CO dissociation number and (b) the TOF value of the nanoparticles with/without C2 models.